



Strain-related differences in antibody-mediated changes in gene expression are associated with differences in capsule and location of binding

Erin E. McClelland^{a,*}, Arturo Casadevall^b

^a Department of Basic Sciences, The Commonwealth Medical College, 525 Pine Street, Scranton, PA 18509, USA

^b Department of Microbiology and Immunology, Albert Einstein College of Medicine, 411 Forchheimer, 1300 Morris Park Avenue, Bronx, NY 10461, USA

ARTICLE INFO

Article history:

Received 24 September 2011

Accepted 24 January 2012

Available online 1 February 2012

Keywords:

mAb 18B7

Capsule

Gene expression profile

Microarray

ABSTRACT

We recently established that antibody (Ab)-binding can induce gene expression changes in a serotype A strain (H99) of the pathogenic yeast, *Cryptococcus neoformans*. That study showed that monoclonal antibodies (mAbs) differing in epitope specificity and protective efficacy elicited differences in gene expression. Because many mAbs bind to serotypes A and D strains differently, we now investigate the binding of one mAb to two strains representing these serotypes. Cells of the serotype A strain H99 and the serotype D strain 24067 were incubated with near saturating concentrations of the IgG1 capsule-binding mAb 18B7 or MOPC, an irrelevant mAb matched control. Comparative immunofluorescence analysis of mAb 18B7 binding revealed that it bound closer to the cell wall in H99 than 24067, where it was associated with decreased or increased cell diameter, respectively. A comparison of encapsulated cell compressibility showed that strain 24067 was more compressible than that of strain H99. RNA was extracted and used for gene expression analysis using the *C. neoformans* JEC21 genomic microarray. After 1 h incubation with mAb 18B7, there were just 2 gene expression changes observed with strain 24067 or strain JEC21, unlike the 43 seen with strain H99. After 4 h incubation with mAb 18B7, there were 14 and 140 gene expression changes observed with strain 24067 and JEC21, respectively. Thus, *C. neoformans* strains differ both in the response and the time of response to mAb binding and these differences may reflect differences in the location of Ab binding, Ab-mediated changes in cell diameter and compressibility of the capsular polysaccharide.

© 2012 Elsevier Inc. All rights reserved.

1. Introduction

The human pathogenic yeast *Cryptococcus neoformans* can be grouped into four major serotypes A, B, C, and D. Recently, cryptococcal strains were phylogenetically divided into two species known as *gattii* (serotypes B and C) and *neoformans* (Kwon-Chung and Varma, 2006), with the latter being subdivided into two varieties: *neoformans* (serotype D) and *grubii* (serotype A). *Cryptococcus gattii* serotypes cause disease primarily in immunocompetent hosts while *C. neoformans* varieties *neoformans* and *grubii* primarily cause disease in immunocompromised hosts (Peachey et al., 1998).

Over the past two decades numerous studies from various laboratories have documented that Ab-mediated immunity can protect against experimental *C. neoformans* infection in rodents (reviewed in Casadevall and Pirofski (2005)). Recently, defects in humoral immunity were associated with increased susceptibility to *C. neoformans* in humans (Subramaniam et al., 2009). Abs to

the *C. neoformans* capsule can promote phagocytosis, activate complement, modulate inflammation, inhibit biofilm formation and reduce the shedding of capsular polysaccharide (reviewed in Zaragoza et al. (2009)). In this regard, there is considerable interest in the development of vaccines that protect by eliciting a protective Ab response and in passive Ab therapies as adjuncts of antifungal therapy for cryptococcosis (Datta and Pirofski, 2006; Magliani et al., 2005).

We recently reported microbial gene expression changes upon Ab binding to strain H99, a serotype A strain (McClelland et al., 2010). That work revealed a previously unsuspected action for Ab-mediated immunity whereby Ab could directly modulate microbial metabolism. A recent study has shown that antibody can also induce gene expression changes in the bacterium *Streptococcus pneumoniae* (Yano et al., 2011), suggesting that this phenomenon is generalizable and applicable to other microbes. With regards to *C. neoformans*, because there are epitope differences in the capsule between serotypes A and D, we investigated whether the effects described previously after the binding of the IgG1 mAb 18B7 to a serotype A strain were applicable to a serotype D strain. The mAb 18B7 has been extensively studied and was evaluated clinically for use on patients with cryptococcosis (Larsen et al., 2005). It

* Corresponding author. Fax: +1 570 504 9660.

E-mail addresses: emcclelland@tcmedc.org (E.E. McClelland), casadevall@aecom.yu.edu (A. Casadevall).

was shown to bind to all four serotypes of *C. neoformans* with higher agglutination in serotype A strains compared to serotype D strains (Casadevall et al., 1998). mAb 18B7 binds to both serotypes A and D strains in an annular immunofluorescence pattern that is associated with Ab-mediated protection (Nussbaum et al., 1997). Whereas our previous study analyzed the effect of different mAbs on one strain of *C. neoformans*, this study analyzed the response of different strains to a single mAb. In contrast to the prior study, which revealed that a single strain responded differently to different mAbs, we now report that two strains from serotypes A and D respond very differently to capsule binding mAb. These data raise the intriguing possibility that the *C. neoformans* serotypes A and D respond differently to the host immune response.

2. Methods

2.1. Strains

C. neoformans strains H99 (serotype A), 24067 (serotype D) or JEC21 (serotype D) were grown from frozen stocks in Yeast Peptone Dextrose (YPD) media for 24–36 h (mid-log phase) at 37 °C and then washed three times with phosphate buffered saline (PBS). Approximately 4×10^7 cells were aliquoted into a 6-well plate and allowed to settle to the bottom of the plate for 10–30 min at room temperature. mAb was then added to the cells slowly, so as not to disturb the cell monolayer and promote aggregation.

Strain 24067, known as 52D, was originally isolated from a case of human cryptococcosis. This strain was used because prior experiments with antibody efficacy have used this strain (Mukherjee et al., 1992, 1993a,b, 1994a,b; Zebedee et al., 1994).

2.2. Antibodies

The mAbs used in the experiments were 18B7 (a *C. neoformans* capsule-specific IgG1) and the control irrelevant mouse IgG1, MOPC. The IgG1 mAb 18B7 was used because it is protective and was used in a human trial of passive therapy for cryptococcosis (Larsen et al., 2005). A near saturating mAb concentration (333 µg/ml) was used for the mAbs 18B7 and MOPC to ensure that all binding sites were occupied (Macura et al., 2007). Using immunoglobulin and glucuronoxylomannan (GXM) molecular masses, we calculated that this concentration corresponded to an IgG1:GXM molar ratio of 1:14. However, we note that even at this relatively high mAb concentration, the capsule is probably not fully saturated because soluble GXM can bind 11 molecules of mAb for each polysaccharide molecule (Janda and Casadevall, 2010). For polysaccharide molecules assembled into an intact capsule such saturation ratios are not achievable, possibly because many of the binding sites are not accessible due to steric hindrance or poor mAb penetration.

2.3. Immunofluorescence microscopy

The mAb 18B7 was directly conjugated to AlexaFluor 488 with the AlexaFluor 488 labeling kit from Invitrogen (Carlsbad, CA). H99 and 24067 were grown from frozen stocks for 2–3 days at 37 °C in YPD broth and then washed three times with PBS. The cells were counted and 5×10^6 cells/ml were aliquoted into microcentrifuge tubes. The cells were blocked with PBS containing 1% bovine serum albumin (BSA) and 0.5% goat serum for 1 h at 37 °C and then washed twice with PBS. *C. neoformans* cells were then incubated with near saturating concentrations of AlexaFluor 488-18B7 and 50 µg/ml calcofluor white (cell wall stain) for 45 min at 37 °C and then washed three times with PBS. The cells were resuspended

in mounting media (50% PBS, 50% glycerol, 0.05 M N propyl gallate) and added to polypropylene slides.

Images and 3-dimensional z-series were taken on 3–5 cells using 0.25 µm slices on an AOBS Leica Confocal microscope. Z-series were reconstructed and analyzed using the free software ImageJ (v1.37, National Institutes of Health) and Voxx (v2.09d, Indiana University). Fluorescence profiles of the equatorial plane of each cell were generated using ImageJ and copied into Microsoft Excel (2003) where they were graphed and the widths of mAb 18B7 binding were measured.

2.4. Measurement of Ab-bound cell diameter

The irrelevant control mAb MOPC was directly conjugated to AlexaFluor 488 and immunofluorescence was done as above with mAb 18B7 plus calcofluor white, mAb MOPC plus calcofluor white or calcofluor white alone. mAb concentrations were near saturating and the concentration of calcofluor white was 50 µg/ml. Twenty-five images of individual cells of each group were taken at the equatorial plane using an AOBS Leica Confocal microscope. Fluorescence profiles were calculated using ImageJ for each image and the diameter of the cell wall was measured as the distance between calcofluor white peaks.

2.5. Capsule compression and diameter studies

H99 and 24067 cells were grown from frozen stocks for 2–3 days at 37 °C in YPD broth and washed three times with PBS. The cells were counted and 1×10^7 cells/ml were aliquoted into hematocrit tubes (75 mm × 1.1 mm). For capsule compression studies, tubes were sealed using two different methods. Four experiments were done where the end of the hematocrit tube was sealed by flame and two experiments were done using candle wax to seal the end of the tube. The open end of the hematocrit tubes was wrapped with parafilm to prevent evaporation and the cells were allowed to settle by gravity overnight. The next day the tubes were centrifuged in a hematocrit centrifuge for 10 min at 4000 rpm. A digital camera was used to photograph the hematocrit tubes prior to and immediately after centrifugation, and the change in cryptococcal column dimensions was measured. For each experiment, 4–6 hematocrit tubes were measured. Adobe Photoshop (v7) was used to measure the distance the cells compressed in mm. Because the cell size of 24067 is significantly more heterogeneous than that of H99, the results were analyzed by dividing the cell distance after centrifugation by the cell distance before centrifugation, yielding the distance compressed for each experiment.

For capsule diameter studies, 1×10^7 cells/ml were aliquoted into hematocrit tubes (75 mm × 1.1 mm), hematocrit tubes were sealed with candle wax and centrifuged in a hematocrit centrifuge for 10 min at 4000 rpm. Capsule diameter was measured before and after centrifugation on 50 cells of each strain. This experiment was done twice with similar results.

2.6. Microarray

The experimental design and the data for the microarray have been deposited in NCBI's Gene Expression Omnibus (Edgar et al., 2002) and are now accessible through GEO Series accession number GSE35241 (<http://www.ncbi.nlm.nih.gov/geo/query/acc.cgi?acc=GSE35241>). Cells and mAbs were incubated at 37 °C for 1, 2 or 4 h, RNA was extracted (RNAeasy Kit, Qiagen, Valencia, CA) and genomic DNA was removed (Message Clean Kit, GenHunter, Nashville, TN). Multiple different pools of RNA were analyzed at Washington University (Table 1), using the *Cn* JEC21 genomic microarray, which was developed by the Cryptococcus Community

Table 1

Summary of the number of genes with >2-fold changes in gene expression and validated with Q-PCR at each microarray timepoint.

Strain	Serotype	mAb	Incubation time at 37 °C (h)	No. of genes identified >2-fold 18B7 vs. MOPC	No. of genes validated with Q-PCR	Reference
24067	D	18B7	1	2 Down-regulated	2 (3 Genes tested)	This study
		MOPC	1			
		18B7	2	6 Down-regulated	2 (4 Genes tested)	This study
		MOPC	2			
JEC21	D	18B7	4	14 Down-regulated	5 (5 Genes tested)	This study
		MOPC	4			
		18B7	1	2 Up-regulated	1 (2 Genes tested)	This study
		MOPC	1			
H99	A	18B7	2	16 Up, 3 down	6 (9 Genes tested)	This study
		MOPC	2			
		18B7	4	140 Down-regulated	12 (42 Genes tested)	This study
		MOPC	4			
H99	A	18B7	1	4 Down, 38 up	11 (14 Genes tested)	McClelland et al. (2010)
		MOPC	1			

Microarray Consortium with financial support from individual researchers and the Burroughs Wellcome Fund. The array includes 7775 probes in duplicate. Briefly, at least two different pools of JEC21 or 24067 RNA made from cells incubated with mAb 18B7 or the control mAb MOPC were each labeled with Cy3 and Cy5 and then hybridized against each other, resulting in two independent biological replicates and two technical replicates (four slides) for each strain at each timepoint. The microarray slides were scanned immediately after hybridization on a ScanArray Express HT Scanner (Perkin Elmer, San Mateo, CA) to detect Cy3 and Cy5 fluorescence. Laser power was kept constant and photomultiplier tube values were set for optimal intensity with minimal background. An additional scan (low PMT) was done for each slide with the PMT such that <1% of the elements were saturating in order to characterize spots which were saturated at the higher PMT setting. Gridding and analysis of images was performed with ScanArray Software Express V2.0 (Perkin Elmer, San Mateo, CA).

For the microarray data of *C. neoformans* strain 24067 incubated with mAb 18B7 or MOPC for 1 h, the gene expression data were averaged across the RNA pools and analyzed (GeneSpring 7.2, Agilent, Redwood City, CA) taking into account the local background intensity and the Cy3/Cy5 dye swap. Twenty percent of the data were used to calculate the Lowess fit at each point and then a Lowess curve was fit to the log-intensity vs. log-ratio plot. After this, the mean signal to Lowess-adjusted controlled ratios was calculated. The cross-chip averages were derived from the antilog of the mean of the natural log ratios across the two microarrays. The data were then filtered in the following manner. First, oligonucleotide elements that received a “present” call by the ScanArray software in half of the high PMT scans in either dye were identified for each condition and all others were excluded from the analysis. Second, the data were filtered for genes in which the mean of the replicates had >2-fold change and $p < 0.05$. The Benjamini & Hochberg false discovery rate for multiple testing corrections was then done for all genes showing changes in gene expression ($p < 0.01$).

For the microarray data of *C. neoformans* strains JEC21 or 24067 incubated with mAb 18B7 or MOPC for 1, 2 or 4 h, the gene expression data were analyzed as follows. Background subtracted raw intensity values were extracted from the .gpr files from each of the channels. The box plots showed minimum variability of the expression values and therefore no normalization was required. The data has been transformed into two-class unpaired data format as required by Significance Analysis of Microarrays (SAM) software. Two files corresponding to strain 24067 at time course of 2 h and 4 h that offered comparison between 18b7 and MOPC types

have been created. Similarly, three files corresponding to time course 1, 2 and 4 h that offered comparison between 18b7 and MOPC types were created for strain JEC21. Using *t*-statistic as the test statistic, 100 random permutations, k-Nearest neighbor imputer and 10 neighbors, we selected probes with false discovery rate 0 or an insignificant value.

2.7. Real-time Q-PCR

RNA was made from log-phase serotype D strains 24067 or JEC21 incubated with near saturating concentrations of mAb 18B7. cDNA was made from two pools of RNA (Quantitech Reverse Transcription kit, Qiagen) and real-time Q-PCR was done using SYBR Green (Applied Biosystems), cDNA and primer in an ABI PRISM® 7900HT Sequence Detection System (Applied Biosystems). Each cDNA was done in quadruplicate, normalized with actin and glycerol-3-phosphate dehydrogenase and the fold change was determined (Pfaffl, 2001). Fold change for mAb 18B7 was relative to the control mAb, MOPC. Real-time Q-PCR was repeated twice.

2.8. Statistics

The width of fluorescence binding in the cryptococcal capsule after mAb 18B7 binding was measured for each cell and then averaged for each mAb concentration used. The Student's *t*-test was then used to test for statistical significance at $p < 0.05$. For measurement of Ab-bound cell diameter, a Tukey–Kramer means comparison was done for all pairs to calculate statistical significance between the pairs at $p < 0.05$. For the centrifugal packing studies, the percentage compressed for all six experiments were averaged and the Student's *t*-test was used to calculate statistical significance at $p < 0.05$. For capsule diameter studies, a multivariate analysis of variance with simple effects was used to test for differences in capsule diameter by strain before and after centrifugation. $p < 0.05$ was considered significant.

3. Results

To establish the pattern of mAb binding to strain 24067 vs. H99, 18B7-AlexaFluor 488 was incubated with cells of each strain for 1 h at 37 °C and then visualized with direct immunofluorescence. mAb 18B7 bound to strain 24067 in a diffuse pattern across the capsule (Fig. 1a). This pattern was different from the compact shell-like binding pattern observed when mAb 18B7 bound to H99 (Fig. 1b).

To establish the location of mAb 18B7 binding on the capsule, the fluorescent profiles of strains H99 and 24067 after 18B7-Alexa-

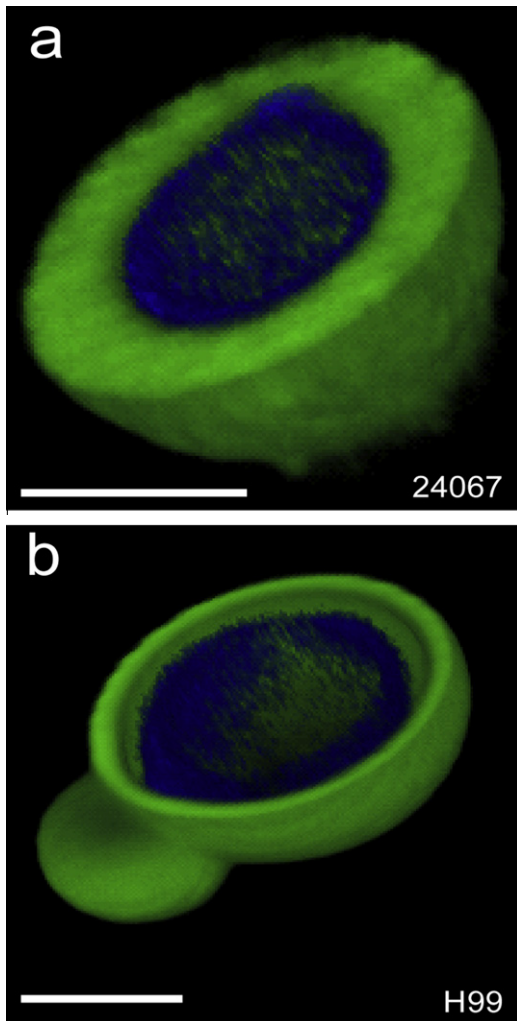


Fig. 1. 3-D reconstructions of mAb 18B7 binding to 24067 (a) and H99 (b). *C. neoformans* cells were incubated with near-saturating concentrations of AlexaFluor 488-conjugated mAb 18B7 (indicated in green) and the cell wall stain calcofluor white (indicated in blue). Cells were washed and mounted for visualization and analysis. Images and 3-dimensional z-series were taken on 3–5 cells using 0.25 μm slices on an AOBs Leica Confocal microscope and analyzed using ImageJ (v1.37, National Institutes of Health) and VoxX (v2.09d, Indiana University). Scale bar is 5 μm . (For interpretation of the references to color in this figure legend, the reader is referred to the web version of this article.)

Fluor 488 binding were analyzed. mAb 18B7 binding to 24067 showed a significantly wider fluorescent intensity profile compared to H99 (4.67 vs. 2.72 μm , $p < 0.004$, Fig. 2a). The fluorescent intensity profile of the equatorial plane of one cell of H99 or 24067 bound to 18B7 is graphically demonstrated in Fig. 2b.

To evaluate whether Ab binding to the capsule affected cell wall geometry we measured the radii of *C. neoformans* cells in the presence or absence of mAb 18B7 after staining with calcofluor white. mAb 18B7 binding to the H99 capsule was associated with a significant reduction of the cell wall radius compared to H99 bound by the control mAb MOPC (17.6 vs. 19.9 μm , $p < 0.05$, Fig. 3a) while mAb 18B7 binding to the capsule of strain 24067 showed a small increase in the average cell radius compared to 24067 bound by the control mAb MOPC (19.8 vs. 18.5 μm , $p < 0.05$, Fig. 3b).

We hypothesized that Ab binding to the capsule could impose a torsional stress on the cell wall and consequently attempted to gain insight into the stiffness of the capsule of the two strains. For a measure of stiffness we analyzed pellet compressibility after sedimentation given that much of the volume of the pellet is deter-

mined by the cryptococcal capsule. In this assay the stiffer capsules would be least compressible and this could be inferred by measuring the change in the dimensions of the pellet after prolonged centrifugation. Comparing the distance traveled by packed cells of strains H99 and 24067 after centrifugation revealed that cells of strain 24067 could be packed into a smaller space by centrifugal forces (0.64 vs. 0.75 ratio of distance compressed, $p = 0.0169$, Fig. 4). We interpreted the higher compressibility of strain 24067 relative to strain H99 as indicating that the capsule of 24067 was less rigid.

If strain 24067 compresses more than H99, then capsule diameter of 24067 should be smaller after centrifugation. To evaluate this hypothesis, we measured the capsule diameter of H99 and 24067 before and after centrifugation. As expected, the capsule diameter of strain 24067 was significantly smaller after centrifugation (1.08 vs. 1.68 μm , $p < 0.001$, Fig. 5). Interestingly, the capsule diameter of strain H99 was significantly larger after centrifugation (2.06 vs. 1.66 μm , $p < 0.02$, Fig. 5).

Given that we observed gene expression changes when mAb 18B7 bound the serotype A strain H99 (McClelland et al., 2010), we used microarray analysis to determine if the same gene expression changes were observed upon mAb 18B7 binding two serotype D strains. While 43 different genes were up- or down-regulated >2-fold in strain H99 upon incubation with saturating concentrations of mAb 18B7 relative to cells incubated with a saturating concentration of an isotype matched control mAb MOPC after 1 h of incubation (McClelland et al., 2010), there were only 2 genes down-regulated >2-fold in strain 24067 and two genes up-regulated >2-fold in strain JEC21 when incubated with saturating concentrations of mAb 18B7 relative to cells incubated with the isotype matched control mAb MOPC after 1 h of incubation (Table 1). Real time Q-PCR confirmed expression changes in both genes down-regulated in strain 24067 and 1 of the 2 genes up-regulated in strain JEC21 (Table 1 and Supplemental Table S1).

Because this is substantially less than the number of genes changed upon mAb 18B7 binding to H99, we tested whether longer incubation times would increase the number of genes changed in serotype D strains. When mAb 18B7 bound to strain 24067 for 2 h, six genes were down-regulated >2-fold, while 14 genes were down-regulated >2-fold after 4 h, relative to cells incubated with the isotype matched control mAb MOPC (Table 1). Real time Q-PCR confirmed expression changes in 2 of 4 genes tested when mAb 18B7 bound to strain 24067 for 2 h and 5 of 5 genes tested when mAb 18B7 bound to strain 24067 for 4 h (Table 1 and Supplemental Table S1). When mAb 18B7 bound to strain JEC21 for 2 h, 16 genes were up-regulated and 3 genes down-regulated >2-fold, while 140 genes were down-regulated >2-fold after 4 h of incubation, relative to cells incubated with the isotype matched control mAb MOPC (Table 1). Real time Q-PCR confirmed expression changes in 6 of 9 genes tested when mAb 18B7 bound to strain JEC21 for 2 h and 12 of 42 genes tested when mAb 18B7 bound to strain JEC21 for 4 h (Table 1 and Supplemental Table S1).

4. Discussion

We have previously shown that mAbs differing in epitope specificity and protective efficacy elicit different gene responses from a *C. neoformans* serotype A strain (McClelland et al., 2010). Because of the known differences between *C. neoformans* serotypes A and D in capsule structure, we investigated whether there would be differences in the effects of mAb binding between the two serotypes. Here we show that the effect of mAb on fungal gene expression is not only dependent on the mAb used but is also a function of the target cell.

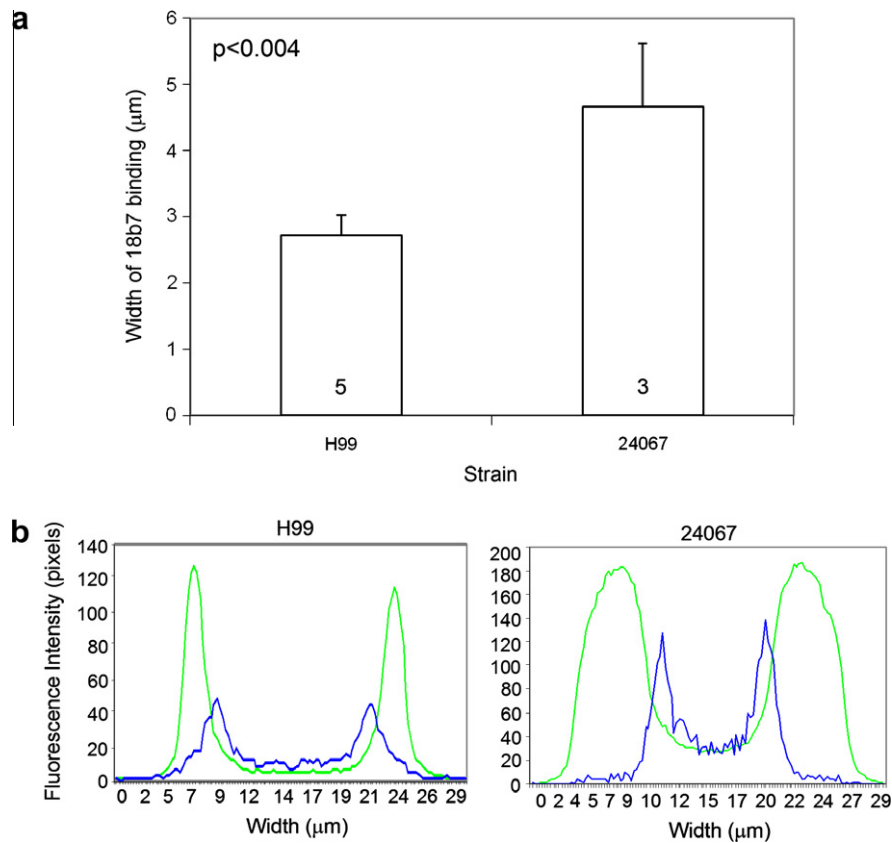


Fig. 2. Width of mAb 18B7 binding H99 or 24067. (a) Bar graph showing average width of mAb 18B7 binding to H99 and 24067. (b) Graphical depiction of the fluorescent intensity profile of one cell that was used to measure width of mAb 18B7 binding to H99 and 24067. *C. neoformans* cells were incubated with near-saturating concentrations of AlexaFluor 488-conjugated mAb 18B7 (indicated in green) and the cell wall stain calcofluor white (indicated in blue). Cells were washed and mounted for visualization and analysis. Images and 3-dimensional z-series were taken on 3–5 cells using 0.25 μm slices on an AOBs Leica Confocal microscope and analyzed using ImageJ (v1.37, National Institutes of Health) and Voxx (v2.09d, Indiana University). Fluorescence profiles of the equatorial plane of each cell were generated using ImageJ and graphed using Microsoft Excel (2003), where the widths of mAb 18B7 binding were measured. Error is standard deviation of the mean. Numbers within bars are the numbers of individual cells measured in each group. (For interpretation of the references to color in this figure legend, the reader is referred to the web version of this article.)

In contrast to the serotype A strain H99, the serotype D strains 24067 and JEC21 were barely responsive to Ab-binding to its capsule with regards to changes in gene expression after 1 h of incubation. In investigating possible differences responsible for this effect we focused on the location of mAb 18B7 binding to the cryptococcal capsule. mAb 18B7 binding to strain H99 was localized primarily to an area near the cell wall. In contrast, for strain 24067 most of the mAb 18B7 bound throughout the capsule in a more diffuse pattern. For H99, mAb 18B7 binding was associated with a significant reduction in cell diameter providing evidence for mechanical changes in yeast cell characteristics. In contrast, for strain 24067, mAb 18B7 binding was associated with a small increase in the cell diameter. To our knowledge this is the first demonstration that antibody binding can alter the physical dimensions of a microbial cell. Small changes in polysaccharide structure caused by Ab binding could result in the propagation of molecular forces to the cell wall. There are at least 4.5×10^8 molecules of GXM/cell in the H99 polysaccharide capsule (Bryan et al., 2005) and 8.6×10^7 mAb 18B7 binding sites/cell (Dadachova et al., 2007). The ratio of mAb:GXM binding sites in the capsule is much lower than the 11:1 ratio measure for GXM in solution (Janda and Casadevall, 2010), suggesting that many sites in the assembled capsule are not accessible to mAb. In saturating conditions, mAb binding to capsular polysaccharide could conceivably produce forces capable of triggering polysaccharide conformational changes that deform cell wall architecture and trigger stress sensors that in turn lead to changes in gene expression. In this regard, there are a number of cell wall membrane proteins that act as mechanosensors, and

it is conceivable that mAb binding in close proximity to the cell wall triggers them. For example, in *Saccharomyces cerevisiae*, the proteins Wsc1 and Mid2 function to convey mechanical pressure information to the cell that can trigger changes in gene expression through the cell wall integrity signaling pathway (Philip and Levin, 2001). Because the Wsc1 protein has homologs in *C. neoformans* strain H99, changes in the cell wall resulting from Ab binding to the capsule may be sufficient to activate signal transduction cascades that manifest themselves in changes in gene expression. In this regard, the larger cell diameter contraction observed after mAb 18B7 binding to strain H99 may be a more powerful signal for mechanoreceptors than the small cell diameter increase observed for strain 24067. Because strain JEC21 does not have Wsc1 homologs and no mechanosensor genes were identified in the microarray data (Table S2), this suggests that the observed gene expression changes seen in the serotype D strains may be due to a different mechanism.

We also considered the possibility that differences in strain responses were due to differences in capsule stiffness. Here we hypothesized that differences in stiffness could result in differences in mechanical tension resulting from mAb binding being transmitted to the cell wall. Sedimentation studies revealed that strain 24067 cells were more compressible than those of strain H99. In concordance with that finding, capsule diameter of strain 24067 was found to be smaller after centrifugation than the capsule diameter of H99, which was paradoxically larger after centrifugation. We have no explanation for why the capsule of strain H99 was larger after centrifugation but we do not feel this curiosity

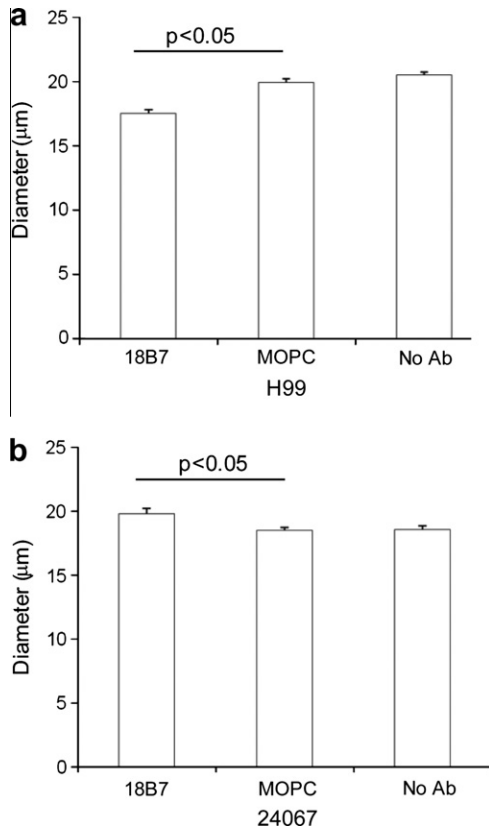


Fig. 3. Graph of the average cell diameters of 25 cells of H99 (a) and 24067 (b) when bound by mAbs 18B7, the control mAb MOPC or no mAb at all. *C. neoformans* cells were incubated with near-saturating concentrations of AlexaFluor 488-conjugated mAb 18B7 and the cell wall stain calcofluor white, AlexaFluor 488-conjugated mAb MOPC and the cell wall stain calcofluor white or calcofluor white alone. Cells were washed and mounted for visualization and analysis. Images and 3-dimensional z-series were taken on 25 cells using 0.25 μm slices on an AOBs Leica Confocal microscope. Fluorescence profiles at the equatorial plane were calculated for each image using ImageJ and the diameter of the cell wall was measured as the distance between calcofluor white peaks.

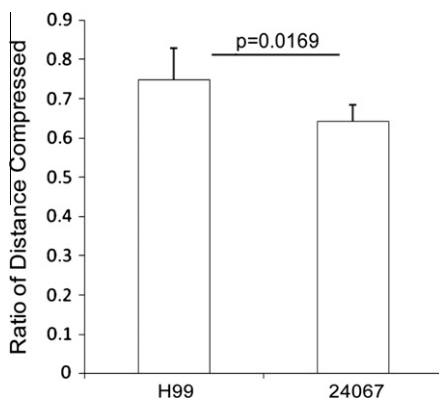


Fig. 4. Graph showing average distance compressed in H99 and 24067 cells. *C. neoformans* cells were aliquoted into hematocrit tubes and allowed to settle by gravity overnight. The next day the tubes were centrifuged and a digital camera was used to photograph the hematocrit tubes prior to and immediately after centrifugation. Adobe Photoshop (v7) was used to measure the change in cryptococcal column dimensions (the distance the cells compressed in mm). Because the cell size of 24067 is significantly more heterogeneous than that of H99, the results were analyzed by dividing the cell distance after centrifugation by the cell distance before centrifugation, yielding the distance compressed for each experiment.

impacts our findings or their interpretation. It is also conceivable that the pressure imparted upon the capsule by sedimentation

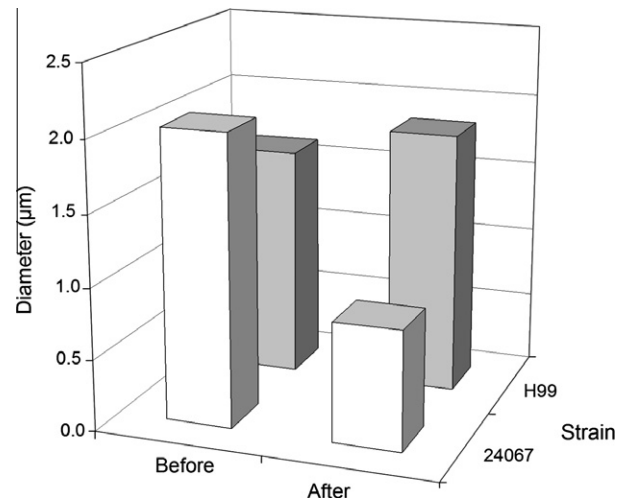


Fig. 5. Effects of centrifugation on capsule diameter of H99 or 24067. *C. neoformans* cells were aliquoted into hematocrit tubes and centrifuged. Capsule diameter was measured before and after centrifugation on 50 cells of each strain. This experiment was done twice with similar results. White bars are strain H99, gray bars are strain 24067.

compression results in changes to the capsular polysaccharide architecture and/or changes in hydration that translate into larger volumes when the pressure is removed as the cells are suspended in solution. Because most of the volume of *C. neoformans* cells is made up of capsule, a higher compressibility and smaller capsule diameter can be interpreted to mean less polysaccharide rigidity. A stiffer polysaccharide capsule combined with closer binding of mAb to the cell wall can be interpreted to mean that mAb-mediated distortions in polysaccharide structure as a result of immunoglobulin binding are more likely to cause cell wall stress that could be sensed by the cell. Ab binding to the *C. neoformans* capsule is known to mediate changes in cell charge and the ability of the polysaccharide to interact with complement receptors (Zaragoza and Casadevall, 2006), thus implying changes in conformation that could translate into cell wall stress. Consistent with this notion is the observation that mAb 18B7 binding to cells of strain H99 caused a reduction in the average radii of the fungal cell wall compared to a small increase in the average radii of the fungal cell wall when 24067 cells were bound by mAb 18B7.

Remarkably, while mAb binding to the *C. neoformans* capsule was associated with many changes in fungal gene expression in the serotype A strain, only two genes manifested changes in mRNA expression >2-fold in the serotype D strains 24067 or JEC21 after 1 h of incubation. After 4 h of incubation with mAb 18B7, strain 24067 showed 14 genes down-regulated >2-fold, while strain JEC21 showed 140 genes down-regulated >2-fold, suggesting that serotype D strains take longer to respond to mAb binding. The differences in gene expression response cannot be attributed to differences in the number of binding sites because Scatchard analysis of mAb 18B7 binding to H99 and 24067 cells revealed that both strains have a comparable number of immunoglobulin binding sites (Dadachova et al., 2007). Additionally, the number of genes showing >2-fold expression changes is similar to that seen in other microarray studies looking at a variety of different responses including heat shock (Kraus et al., 2004), gene expression during macrophage infection (Fan et al., 2005), response to blue-light (Idnurm and Heitman, 2010), genes involved in signal transduction (Maeng et al., 2010) and response to carbon dioxide (Kim et al., 2010).

To get a better idea of the specific response of the serotype D strains 24067 and JEC21 to binding by mAb 18B7 and because there were so few genes showing >2-fold changes in expression,

we broadened our analysis to include all genes with statistically significant changes (Table S2). When we classified these genes according to their functional role, we observed an overall picture of the down-regulation of transcription, translation and metabolism over time, with more down-regulation seen with longer incubation times. We also investigated whether any of the 43 genes whose expression was altered in strain H99 by mAb 18B7 binding were also changed in strains JEC21 or 24067. Interestingly, only three genes were changed that were common between the serotypes A and D strains: CND03490 (mannoprotein MP98), CND00530 (urea transporter), and CNJ02710 (membrane protein). This data suggests that there is a different response to mAb 18B7 binding by serotypes A and D strains.

Finally, while the microarray data describe an overall picture of the down-regulation of most house-keeping functions of the cell, the phenotypic changes we report in strain 24067 after mAb 18B7 binding were observed after only 45 min to 1 h of incubation with mAb 18B7, suggesting that these results are largely independent of the down-regulation of transcription, translation and metabolism and instead may be due to innate differences between the serotypes.

In summary, our results show that the gene expression response of *C. neoformans* in reaction to Ab binding can differ greatly depending on the strain and that serotype D strains seem to have a longer response time than serotype A strains. Historically, it has been easier to demonstrate Ab-mediated protection against serotype D strains than serotype A strains in mouse models of infection (Mukherjee et al., 1995). Although we can make no conclusions regarding an association between Ab responsiveness and Ab-mediated protection given the relatively few strains examined, the findings are intriguing and suggest new avenues for investigation. In this study we associated strain-related differences in their response to Ab binding with differences in the locations of the mAb epitopes between the two serotypes, as well as differences in cell diameter and in the compressibility and size of the capsule. Our findings provide additional evidence that Ab binding by itself can affect microbial physiology, a finding that has now been documented in both *C. neoformans* and the gram positive bacterium *S. pneumoniae* (Yano et al., 2011). This connection between humoral immunity and microbial metabolism provides new opportunities for understanding how the immune system interacts with microbes.

Acknowledgments

We would like to thank Ms. Letizia Hobbs for capsule measurements, Dr. Victor Francone for help with image preparation, and Ms. Mary Ann Kaine for help with the real time Q-PCR. We also thank Seth Crosby, Mike Heinz and Jahangheer Shaik at Washington University St. Louis for their help and analysis of the microarray data. A.C. is supported by the National Institutes of Health Awards AI033142, AI033774 and HL059842-08.

Appendix A. Supplementary material

Supplementary data associated with this article can be found, in the online version, at doi:10.1016/j.fgb.2012.01.006.

References

Bryan, R.A., Zaragoza, O., Zhang, T., Ortiz, G., Casadevall, A., Dadachova, E., 2005. Radiological studies reveal radial differences in the architecture of the polysaccharide capsule of *Cryptococcus neoformans*. *Eukaryot. Cell* 4, 465–475.
 Casadevall, A., Pirofski, L., 2005. Insights into mechanisms of antibody-mediated immunity from studies with *Cryptococcus neoformans*. *Curr. Mol. Med.* 5, 421–433.

Casadevall, A., Cleare, W., Feldmesser, M., Glatman-Freedman, A., Goldman, D.L., Kozel, T.R., Lendvai, N., Mukherjee, J., Pirofski, L.A., Rivera, J., et al., 1998. Characterization of a murine monoclonal antibody to *Cryptococcus neoformans* polysaccharide that is a candidate for human therapeutic studies. *Antimicrob. Agents Chemother.* 42, 1437–1446.
 Dadachova, E., Bryan, R.A., Huang, X., Ortiz, G., Moadel, T., Casadevall, A., 2007. Comparative evaluation of capsular polysaccharide-specific IgM and IgG antibodies and F(ab')₂ and Fab fragments as delivery vehicles for radioimmunotherapy of fungal infection. *Clin. Cancer Res.* 13, 5629s–5635s.
 Datta, K., Pirofski, L.A., 2006. Towards a vaccine for *Cryptococcus neoformans*: principles and caveats. *FEMS Yeast Res.* 6, 525–536.
 Edgar, R., Domrachev, M., Lash, A.E., 2002. Gene Expression Omnibus: NCBI gene expression and hybridization array data repository. *Nucl. Acids Res.* 30, 207–210.
 Fan, W., Kraus, P.R., Boily, M.J., Heitman, J., 2005. *Cryptococcus neoformans* gene expression during murine macrophage infection. *Eukaryot. Cell* 4, 1420–1433.
 Idnurm, A., Heitman, J., 2010. Ferrocyclase is a conserved downstream target of the blue light-sensing white collar complex in fungi. *Microbiology* 156, 2393–2407.
 Janda, A., Casadevall, A., 2010. Circular dichroism reveals evidence of coupling between immunoglobulin constant and variable region secondary structure. *Mol. Immunol.* 47, 1421–1425.
 Kim, M.S., Ko, Y.J., Maeng, S., Floyd, A., Heitman, J., Bahn, Y.S., 2010. Comparative transcriptome analysis of the CO₂ sensing pathway via differential expression of carbonic anhydrase in *Cryptococcus neoformans*. *Genetics* 185, 1207–1219.
 Kraus, P.R., Boily, M.J., Giles, S.S., Stajich, J.E., Allen, A., Cox, G.M., Dietrich, F.S., Perfect, J.R., Heitman, J., 2004. Identification of *Cryptococcus neoformans* temperature-regulated genes with a genomic-DNA microarray. *Eukaryot. Cell* 3, 1249–1260.
 Kwon-Chung, K.J., Varma, A., 2006. Do major species concepts support one, two or more species within *Cryptococcus neoformans*? *FEMS Yeast Res.* 6, 574–587.
 Larsen, R.A., Pappas, P.G., Perfect, J., Aberg, J.A., Casadevall, A., Cloud, G.A., James, R., Filler, S., Dismukes, W.E., 2005. Phase I evaluation of the safety and pharmacokinetics of murine-derived anticryptococcal antibody 18B7 in subjects with treated cryptococcal meningitis. *Antimicrob. Agents Chemother.* 49, 952–958.
 Macura, N., Zhang, T., Casadevall, A., 2007. Dependence of macrophage phagocytic efficacy on antibody concentration. *Infect Immun.* 75, 1904–1915.
 Maeng, S., Ko, Y.J., Kim, G.B., Jung, K.W., Floyd, A., Heitman, J., Bahn, Y.S., 2010. Comparative transcriptome analysis reveals novel roles of the Ras and cyclic AMP signaling pathways in environmental stress response and antifungal drug sensitivity in *Cryptococcus neoformans*. *Eukaryot. Cell* 9, 360–378.
 Magliani, W., Conti, S., Arseni, S., Salati, A., Ravanetti, L., Maffei, D.L., Giovati, L., Polonelli, L., 2005. Antibody-mediated protective immunity in fungal infections. *New Microbiol.* 28, 299–309.
 McClelland, E.E., Nicola, A.M., Prados-Rosales, R., Casadevall, A., 2010. Ab binding alters gene expression in *Cryptococcus neoformans* and directly modulates fungal metabolism. *J. Clin. Invest.* 120, 1355–1361.
 Mukherjee, J., Scharff, M.D., Casadevall, A., 1992. Protective murine monoclonal antibodies to *Cryptococcus neoformans*. *Infect Immun.* 60, 4534–4541.
 Mukherjee, J., Casadevall, A., Scharff, M.D., 1993a. Molecular characterization of the humoral responses to *Cryptococcus neoformans* infection and glucuronoxylomannan–tetanus toxoid conjugate immunization. *J. Exp. Med.* 177, 1105–1116.
 Mukherjee, J., Pirofski, L.A., Scharff, M.D., Casadevall, A., 1993b. Antibody-mediated protection in mice with lethal intracerebral *Cryptococcus neoformans* infection. *Proc. Natl. Acad. Sci. USA* 90, 3636–3640.
 Mukherjee, J., Zuckier, L.S., Scharff, M.D., Casadevall, A., 1994a. Therapeutic efficacy of monoclonal antibodies to *Cryptococcus neoformans* glucuronoxylomannan alone and in combination with amphotericin B. *Antimicrob. Agents Chemother.* 38, 580–587.
 Mukherjee, S., Lee, S., Mukherjee, J., Scharff, M.D., Casadevall, A., 1994b. Monoclonal antibodies to *Cryptococcus neoformans* capsular polysaccharide modify the course of intravenous infection in mice. *Infect Immun.* 62, 1079–1088.
 Mukherjee, J., Scharff, M.D., Casadevall, A., 1995. Variable efficacy of passive antibody administration against diverse *Cryptococcus neoformans* strains. *Infect Immun.* 63, 3353–3359.
 Nussbaum, G., Cleare, W., Casadevall, A., Scharff, M.D., Valadon, P., 1997. Epitope location in the *Cryptococcus neoformans* capsule is a determinant of antibody efficacy. *J. Exp. Med.* 185, 685–694.
 Peachey, P.R., Gubbins, P.O., Martin, R.E., 1998. The association between cryptococcal variety and immunocompetent and immunocompromised hosts. *Pharmacotherapy* 18, 255–264.
 Pfaffl, M.W., 2001. A new mathematical model for relative quantification in real-time RT-PCR. *Nucl. Acids Res.* 29, e45.
 Philip, B., Levin, D.E., 2001. Wsc1 and Mid2 are cell surface sensors for cell wall integrity signaling that act through Rom2, a guanine nucleotide exchange factor for Rho1. *Mol. Cell. Biol.* 21, 271–280.
 Subramaniam, K., Metzger, B., Hanau, L.H., Guh, A., Rucker, L., Badri, S., Pirofski, L.A., 2009. IgM(+) memory B cell expression predicts HIV-associated cryptococcosis status. *J. Infect. Dis.* 200, 244–251.
 Yano, M., Gohil, S., Coleman, J.R., Manix, C., Pirofski, L.A., 2011. Antibodies to *Streptococcus pneumoniae* capsular polysaccharide enhance pneumococcal quorum sensing. *mBio* 2, e00176–e00111.

- Zaragoza, O., Casadevall, A., 2006. Monoclonal antibodies can affect complement deposition on the capsule of the pathogenic fungus *Cryptococcus neoformans* by both classical pathway activation and steric hindrance. *Cell. Microbiol.* 8, 1862–1876.
- Zaragoza, O., Rodrigues, M.L., De Jesus, M., Frases, S., Dadachova, E., Casadevall, A., 2009. The capsule of the fungal pathogen *Cryptococcus neoformans*. *Adv. Appl. Microbiol.* 68, 133–216.
- Zebedee, S.L., Koduri, R.K., Mukherjee, J., Mukherjee, S., Lee, S., Sauer, D.F., Scharff, M.D., Casadevall, A., 1994. Mouse–human immunoglobulin G1 chimeric antibodies with activities against *Cryptococcus neoformans*. *Antimicrob. Agents Chemother.* 38, 1507–1514.